Microwave-assisted wet peroxide oxidation catalyzed by graphite. Effect of salinity

Lucía López Perela

Máster en Ingeniería Química

MÁSTERES
DE LA UAM
2017 - 2018

Facultad de Ciencias

UAM Universidad Autónoma de Madrid

Universidad Rey Juan Carlos

UNIVERSIDAD AUTONOMA DE MADRID

MASTER UNIVERSITARIO EN INGENIERÍA QUÍMICA

Curso académico 2017-18

Trabajo Fin de Máster

Microwave-assisted wet peroxide oxidation catalyzed by graphite. Effect of salinity

Autor: Lucía López Perela

Director: José A. Casas de Pedro, Alicia L. García Costa

Contents

Summary 1

Introduction 3

Objectives 10

Methodology 11

Reagents 11

Reactors 11

Analytical methods 12

Results 13

MW-CWPO optimization 13

Influence of salinity in CWPO and MW-CWPO 19

Kinetics 26

Conclusions 28

References 29

Summary

Water is a scarce resource that, furthermore, results increasingly polluted day to day. The social and environmental concern gives rise to wastewater treatments, such as advanced oxidation processes (AOPs), which exploit the generation of $HO_x^{\bullet}$ radicals. Among them, Catalytic Wet Peroxide Oxidation (CWPO) works at mild conditions using a solid redox catalyst for H_2O_2 decomposition into radicals. Nevertheless, actual trends seek process intensification, via temperature or introduction of an external source of energy. At this point, microwave radiation comes up as an interesting alternative, given its rapid and selective heating. Microwaves (MW) are responsible for enhancing the degradation of some pollutants in systems combining MW and CWPO.

Among advantages of employing MW, there is the reduction of reaction time, increase of the selectivity of reaction, improvement of reaction speed, reduction of equipment size and waste, and increase of products yield and purity. As a result, this study proposes the application of MW-CWPO to treat a phenol-polluted aqueous solution.

The need of addressing seawater treatments evidences the importance of effluents' salinity, which should not compromise its efficiency. In certain processes, salts provoke undesirable scavenging reactions, lowering the efficiency of pollutant removal by reacting with potential oxidants. However, there is no consensus in this subject and, furthermore, impact on MW treatments has not been reported yet.

Consequently, the initial challenge is to study the impact of process variables in MW-CWPO such as pH, temperature, catalyst load and oxidant concentrations in order to find the optimal point to operate. In this research, it is proved that the optimal operating conditions for the removal of 100 $mg \cdot L^{-1}$ phenol are pH_0 3, 120 ºC, 500 $mg \cdot L^{-1}$ graphite and 500 $mg \cdot L^{-1}$ H_2O_2.

Hence, these parameters are then applied in CWPO and MW-CWPO to synthetic brines, with no content of phenol and containing 100 $mg \cdot L^{-1}$ phenol and chloride concentrations ranging from 0 to 40 $mg \cdot L^{-1}$. In these conditions, no chlorinated byproducts are generated. However, in absence of phenol Cl^- concentrations up to 10 $g \cdot L^{-1}$ have a negative effect over H_2O_2 decomposition in CWPO and MW-CWPO. Such effect could be related to H_2O_2-chloride anions competition for catalytic active centers. On the contrary, in

presence of phenol, low Cl^- concentrations enhance H_2O_2 depletion. In these conditions, hot spots seem to avoid adsorption competition.

Regarding TOC mineralization, it is enhanced for CWPO at high [Cl^-], since chlorine is able to act as an oxidant as well. Whereas for MW-CWPO system –except for 40 $g \cdot L^{-1}$– an augmentation of [Cl^-] lowers TOC removal efficiency. Thus, chloride addition has a dual effect. Salinity of the medium can affect positively to the interaction of organic matter with the catalyst, by modifying its adsorption, approaching reactants to catalyst's surface and empowering the reaction. This is what happens in CWPO for all [Cl^-]. However, the use of MW gives rise to a cross-effect due to the presence of hot spots generated over graphite surface. As MW-CWPO worked efficiently before the addition of chloride due to hot spots formation, it has a detrimental impact. The reason is that when chloride anions take part in the reaction, the catalytic redox cycle becomes altered. Chloride anions release electrons, resulting oxidized into chlorine, which can interact with organic matter. This reaction competes with the oxidation of H_2O_2 to $HO_2^{\bullet}$ radicals for active centers of the redox catalyst. Nevertheless, at a sufficiently high [Cl^-], the scavenging effect is overcame by catalyst surface improvement.

In any case, the lowest mineralization, which corresponds to 25 $g \cdot L^{-1}$ Cl^- run, obtained by proposed treatment (i.e. MW-CWPO), comes to 77% TOC removal, being the most unfavorable case. This outstanding result means that this process represents a feasible alternative to remove pollutants in aqueous phase in spite of the presence of salts in it.

Finally, H_2O_2 decomposition follows a pseudo-first order, with an apparent rate constant around 0.13 min^{-1} in CWPO and 0.14 min^{-1} in MW-CWPO, whereas TOC mineralization follows a pseudo-second order with an apparent rate constant of $1.54 \cdot 10^{-3}$ $L \cdot min \cdot mg^{-1}$ and $2.38 \cdot 10^{-3}$ $L \cdot min \cdot mg^{-1}$, respectively. Thus, even though H_2O_2 has a similar decomposition rate, organic matter removal is greatly enhanced when coupling MW to CWPO due to the non-thermal effects such as the hot spots formation on the surface of graphite.

Introduction

Nowadays, the presence of persistent pollutants from industrial activities in seawater is a notorious concern. Moreover, the increasing demand of water, along its scarcity as a resource, has arisen a growing interest on the study of its misuse and treatment. Advanced oxidation processes (AOPs) have been widely studied as wastewater treatment methods, and result highly effective for organic pollutants removal (N. Remya 2011). AOPs typically involve the generation and use of hydroxyl and hydroperoxyl radicals ($HO_x^{\bullet}$). These are strong oxidizing agents, which are able to destroy compounds that cannot be removed by conventional wastewater treatment plants or chemical methods with oxidants such as oxygen, ozone or chlorine.

Different oxidation processes, such as wet air oxidation (WAO) and catalytic wet air oxidation (CWAO), have been used to treat phenol-containing industrial wastewaters. However, high pressures (20-200 bar) and temperatures (200-320 ºC) are needed, which increase the treatment cost (Pintar 2003).

An alternative, in order to reduce the severity of these operation conditions, is the use of AOPs, among which hydrogen peroxide (H_2O_2) acts as a source of $HO_x^{\bullet}$ radicals. In this sense, the Fenton process is one of the most representatives. Driven by a redox cycle between H_2O_2 and Fe^{2+}at pH around 3, as shown in Eq. 1-Eq. 2, it is known for its capability of working efficiently at mild conditions and using environmentally friendly reactants (Fenton 1894).

$$Fe^{2+} + H_2O_2 \rightarrow Fe^{3+} + HO^- + HO^{\bullet} \qquad \textit{Eq. 1}$$

$$Fe^{3+} + H_2O_2 \rightarrow Fe^{2+} + HO_2^{\bullet} + H^+ \qquad \textit{Eq. 2}$$

The main drawback of the process is the difficulty to recover the catalyst after reaction. In order to overcome this issue, solid catalysts are employed in the so-called catalytic wet peroxide oxidation (CWPO) (E. Guélou 2003). Typically, these catalysts are formed by a metallic active phase (Fe or Cu) supported on activated carbon, alumina or pillared clays. (J. A. Zazo 2006), (M. Munoz 2013), (C.B. Molina 2010).

Nevertheless, given the low operating pH, active phase may leach, polluting the effluents. Thus, recent research also explores the use of bare carbon materials as catalysts such as active carbon, graphite or carbon black. These present a lower activity but higher stability in relation to iron-based catalysts (C.M. Dominguez 2013), (C. M. Dominguez 2014).

The actual trend in AOPs is the process intensification, whose aim is to obtain higher mineralization rates or enhance the catalyst lifetime (G. Pliego 2015). AOP intensification is usually performed by increasing the temperature or introducing an external source of energy, such as UV-Vis radiation or ultrasounds. In addition, Microwave (MW) radiation has lately attracted attention as an efficient alternative in this field, given its rapid and selective heating (N. Wang 2016).

MW is a part of the electromagnetic spectrum occurring in the frequency range of 300 MHz to 300 GHz. The heating mechanism, unlike conventional thermal sources, goes from the outside to the inside (in most of thermal process heating starts from the interior of the material body), as shown in Figure 1.

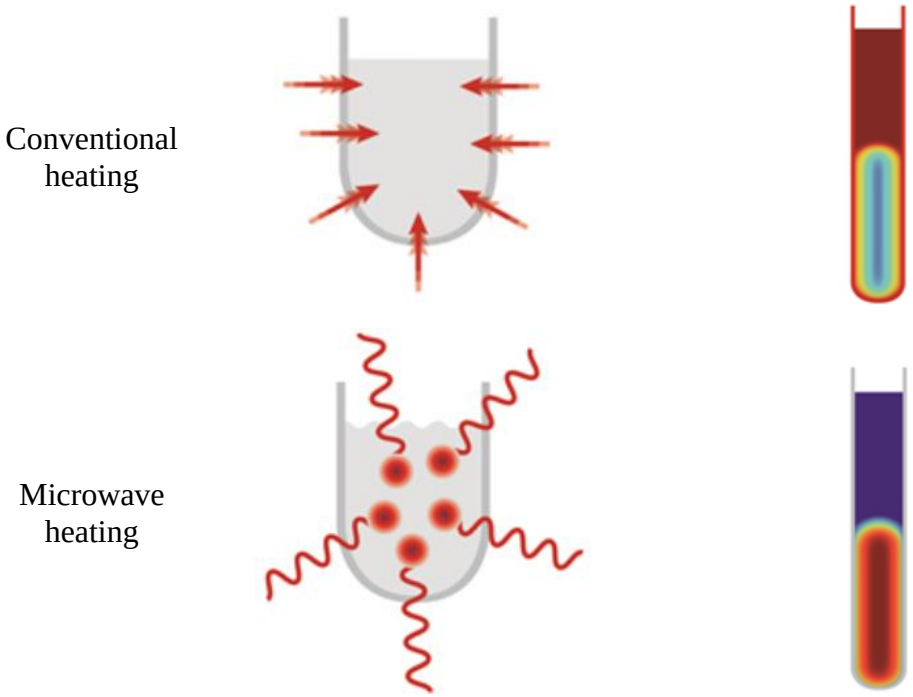

Figure 1. Heating mechanisms and temperatures distributions in two different heat sources.

Furthermore, MW can provide a rapid heating of materials depending on its dissipation factor (tan δ). It is measured as the ratio of relative loss factor (ε") to the dielectric constant (ε') of the material. Relative loss factor accounts for the internal loss mechanisms (amount of MW energy dissipated in the material in form of heat), while the dielectric constant stands as a relative measure of the MW energy density in the material. Therefore, a material with a high ε" is easily heated by MW energy (C.E. George 1994). In relation to MW absorbing properties, materials can be classified as opaque, transparent or absorbent (Sutton 1989). An example of an *opaque* material would be any metal, *transparent* a polytetrafluoroethylene (PTFE) and *absorbent*, graphite.

The basis of MW lies in the fact that it works at a molecular level, since it is an electromagnetic source that cause dipoles to rotate. Thus, energy turns into heat due to molecular friction (S. Lv 2009). Concerning the heating mechanisms of MW, the principal are dipolar polarization, conduction mechanism and interfacial polarization.

- Dipolar polarization results from intermolecular inertia, which is responsible for the majority of MW heating observed in the solvent systems. When the dipole is subjected to a high-frequency alternating electric field of the MW, rotation of the dipole cannot adequately follow the rate of change in direction of the electric field. This leads to a time delay, causing a substantial quantity of energy to turn into heat (H. Hidaka 2007).
- The conduction mechanism happens when MW irradiates an electrical conductor. At that time, the charge carriers (electrons, ions, etc.) move through the material because of the influence of the electric field, which results in a polarization. Subsequently, the induced currents cause the heating of the sample depending on the electrical resistance of the material.
- Interfacial polarization occurs in heterogeneous catalysis. In fact, this mechanism is the responsible factor of improved degradation efficiency. The rapid pollutant degradation in the MW system with a MW-absorbent (like activated carbon) is mainly due to the hot spots formation on its surface, which is a unique mechanism for MW. This is essential to speed-up reactions in many processes. Generally, the delocalized π-electrons in the surface of the AC are free to move. During the MW irradiation, the kinetic energy of electrons on the surface of the AC increases, which enables the electrons to jump out of the material resulting in the formation of hot spots by ionizing the surrounding atmosphere (J.A. Menéndez 2010). These hot spots are actually plasmas, which are confined to a tiny region of space and last for fractions of a second. The temperature of hot spots can ordinarily reach 1200 ºC (D.A. Jones 2002). Hot spots cause thermal effects resulting from the differences between the temperature at the reaction site and temperature in the medium or reactor system. This facilitates the destruction of complex chemical bonds by decreasing the activation energy and increasing the rate of reaction. Furthermore, the quantum energy of MW causes the vibration of molecules, which also helps to decrease the activation energy. Lastly, MW reduce the equipment size and waste (Haque 1999).

Besides, non-thermal effects can also take place in MW systems, such as the electrical effect, magnetic effect, and chemical effect (N. Li 2010), (D.M. Gu 2011), (I. Milosevic 2011). In an aqueous reaction system, the MW non-thermal effects could result in the excitation of reactant molecules to higher vibrational and rotational energy levels, and then the chemical bond of a polar reactant molecule could be weakened. However, despite the large number of publications about the non-thermal effects of MW irradiation, there are still many conflicting results on it (L. Yang 2014) and even the possibility of its existence is still controversial (N. Wang 2016).

Nevertheless, the energy of MW may be sometimes insufficient to disrupt the chemical bonds of many organic compounds (P. Müler 2003). Therefore, combinations between MW, adsorbents, catalysts and AOPs have been tested with the aim of increasing treatment efficiency and shorten reaction time. For instance, the possibility of combining MW with Fenton's reagent seems an interesting alternative. For the Fenton process, optimal pH is approximately 3, since a lower or higher pH in the reaction system would result in the reduction of the wastewater treatment efficiency and a longer duration time. However, the addition of MW irradiation would allow the feasible pH range to be extended to the neutral range and reaction time to be shortened (M. Ravera 2009), (J. Hong 2012), (X.Y. Bi 2012).

The main advantage of combining MW with AOPs is the improvement in the yield of free radical generation from oxidants and rapid polarization of pollutants (L. Zhang 2007). The dipolar polarization mechanism enhances the degradation of various pollutants in the systems combining MW and oxidants. As previously mentioned, this mechanism creates elevated temperature within a shorter span in relation to conventional heating methods, which provokes the increased decomposition of H_2O_2 into $HO^{\bullet}$ as shown in Eq. 3 (E. Cigdem 2008). Subsequently, the $HO^{\bullet}$ generated in the system undergoes adduction reaction with the target pollutants and the resulting intermediates. As a result, reactions show rapid and improved degradation rates (M. Ravera 2009). Nevertheless, H_2O_2 at high concentrations can act as $HO^{\bullet}$ quencher as shown in Eq. 4-Eq. 6, consequently lowering $HO^{\bullet}$ concentration available for oxidizing. This scavenging effect of H_2O_2 causes degradation rates to decrease. Hence, high H_2O_2 dosages may not always amplify the degradation efficiency of the target compounds. Therefore, the optimum dosage of H_2O_2 must be determined to maintain a higher degradation rate as well as to minimize the cost of overall treatment.

$$H_2O_2 \xrightarrow{MW} 2HO^{\bullet} \quad \textit{Eq. 3}$$

$$HO^{\bullet} + H_2O_2 \xrightarrow{MW} HO_2^{\bullet} + H_2O \quad \textit{Eq. 4}$$

$$2HO_2^{\bullet} \xrightarrow{MW} H_2O_2 + O_2 \quad \textit{Eq. 5}$$

$$HO^{\bullet} + HO_2^{\bullet} \xrightarrow{MW} H_2O + O_2 \quad \textit{Eq. 6}$$

Regarding the catalyst, different supports have been addressed in the literature, such as graphite, AC, carbon black, silicon carbide and carbon nanofibers. Among those, AC has proved to be an efficient material for catalyzing MW assisted wet peroxide oxidation in the mineralization of phenol. AC acts as adsorbent and catalyst in a complex mechanism implying the formation of aromatic condensation by-products, which are adsorbed onto the AC. Then, $HO_x^{\bullet}$ achieve both pollutant oxidation and catalyst partial regeneration, favored by the formation of hot spots on the carbon surface upon MW radiation (A. L. Garcia-Costa 2017). Hence, same technology has been tested for addressing a mix of aromatics typically found in petrochemical wastewaters: benzene, toluene, o-xylene and naphthalene (BTXN) as target pollutants. It has proved to be effective for the degradation of BTXN in aqueous phase achieving complete BTXN depletion and up to 97% Total Organic Carbon (TOC) removal in fairly short time (15 min) at 120ºC, pH_0 3, using H_2O_2 at the stoichiometric dose and AC load at 1 $g \cdot L^{-1}$ (A.L. Garcia-Costa 2016). Furthermore, reactions have been carried out substituting AC by graphite, which has proved to be more stable and equally active.

Regarding graphite, there are two important features in the structure and electronic properties: the two-dimensional (2D) layered structure and the amphoteric character. The latter is featured by the fact that graphite works not only as oxidizer, but also as a reducer in chemical reactions. Both characteristics stem from the zero-gap-semiconductor-type or semi metallic electronic structure (F. Béguin 2009) and are responsible of making it an interesting material on this field.

Summarizing, literature has demonstrated that pollutant degradation treatments based on MW have many advantages. They: (1) reduce the reaction time, (2) increase the selectivity of reaction, (3) decrease the activation energy, (4) improve the speed of reaction, (5) reduce the equipment size and waste, (6) provide ease of control, and (7) increase the yield and purity of products. These advantages are mainly due to thermal and non-thermal effects of MW, i.e. superheating, polarization, dielectric properties, hot spots

formation and nuclear spin rotation and alignment. The combination of MW with AOPs is an emerging trend in wastewater treatment. At the same time, several other operational parameters including pH, MW power, oxidant/catalyst dosage, irradiation time and air supply could influence the performance of MW systems and should be studied (N. Remya 2011).

On the other hand, the possibility of applying this technology to seawater effluents entails the need of studying the influence that the presence of salts could have on the process. There is not a thorough study on this topic; however, it has been reported that salts provoke undesirable scavenging reactions, lowering the efficiency of the process by reacting with potentially oxidant radicals. In fact, some authors have outlined the necessity of applying different technologies to saline wastewater by considering their reduced activity, if taken individually, in treating highly saline effluents (S. Cataldo 2016).

According to literature, at low NaCl concentrations (up to 2.5 $g \cdot L^{-1}$) scavenging effect is not noticed, but lower TOC removals were recorded as salt concentration exceeded 10 $g \cdot L^{-1}$ (R. Maciel 2004). The decrease on process efficiency can be attributed to the presence of chloride ions, since they are able to trap hydroxyl radicals, producing precursors of hypochlorous acid, as shown in Eq. 7. The reaction of hydroxyl radicals with chloride ions can produce chlorine radicals ($Cl^{\bullet}$) that react with hydrogen peroxide, forming chloride ($Cl_2^{\bullet-}$) and $HO_2^{\bullet}$ radicals (Eq. 8 and Eq. 9), which are less reactive. Some possible reactions (Eq. 10 and Eq. 11) of chlorine radicals are shown below (Pignatello 1992), (M.C. Lu 1997).

$$Cl^- + HO^{\bullet} \rightarrow ClHO^- \qquad \textit{Eq. 7}$$

$$Cl^- + HO^{\bullet} \rightarrow Cl^{\bullet} + HO^- \qquad \textit{Eq. 8}$$

$$Cl^{\bullet} + H_2O_2 \rightarrow HO_2{}^{\bullet} + Cl^- + H^+ \qquad \textit{Eq. 9}$$

$$Cl^- + Cl^{\bullet} \rightarrow Cl_2{}^{\bullet-} \qquad \textit{Eq. 10}$$

$$Cl^{\bullet} + Cl^{\bullet} \rightarrow Cl_2 \qquad \textit{Eq. 11}$$

Consequently, the treatment of saline wastes constitutes a challenging issue. For instance, photocatalysis is strongly inhibited by the presence of salts, which decrease the solubility of O_2 and compete with the organic substrates for absorption on surface active sites. On the other hand, O_3 oxidation of polluted seawater results in formation of highly carcinogenic BrO_3^- ions. Furthermore, recent research of the group has proved that the

application of UV or electric potentials to saline effluents with the aim of deploying present organic contaminants yields chlorinated intermediates. The reason for this is the attack of hydroxyl radicals, which activate chloride radicals and subsequently chlorine, which enters the molecule. Nevertheless, in other treatments, namely Fenton reaction at mild conditions, this fact does not happen.

Other researches related to removal of dyes from saline wastewaters claim that the addition of Cl^- has a dual effect on the TOC removal rate. It is enhanced at low concentrations (0-2 g/L), whereas higher amounts reduce further dye decomposition. The enhancement is attributed to a surface chain-transfer mechanism involving chlorine radicals related to substrate adsorption onto the catalyst (R. Yuan 2012).

It seems clear that there are contradictory statements on the topic of treatment of saline wastewaters. Moreover, there is no literature on the topic of MW applied to this kind of wastewaters. Thus, the present work intends to clarify the effect of this variable.

Objectives

The aim of the present work is initially to study the impact of process variables, such as pH_0, temperature and catalyst and oxidant concentrations. These parameters will be slightly varied using previous research as a reference. The point of this is to obtain the optimal operation conditions for phenol oxidation (at 100 $mg \cdot L^{-1}$) from a synthetic aqueous matrix using hydrogen peroxide at stoichiometric amount (500 $mg \cdot L^{-1}$) and graphite as a catalyst in the MW-CWPO process. Reaction intermediates will be analyzed to discard any chance of forming toxic byproducts, apart from tracing the reaction pathway.

After that, the selected optimal conditions will be applied to both CWPO and MW-CWPO of synthetic brines containing phenol. Besides, a multivariable study will also address the interactions between reagents and pollutant, as well as the influence of chloride anion in the medium. Phenomena such as whether chlorine has any influence on the efficiency or it enters the molecule will be analyzed.

Eventually, kinetic models will be developed and fitted to experimental data in order to calculate kinetic constants for this system.

Methodology

Reagents

Phenol (99.9%) was supplied by Sigma-Aldrich and H_2O_2 (30% w/v) by Panreac. Respective aqueous solutions were prepared at pH_0 3 using HCl (37% w/v, Panreac). Graphite (G-S, ref.: 282863) supplied by Sigma-Aldrich was employed as catalyst. Working standard solutions of phenol, catechol, resorcinol, hydroquinone, p-benzoquinone and organic acids (fumaric, malonic, maleic, acetic and formic from Sigma-Aldrich and oxalic from Panreac) were prepared for equipment calibration. H_2SO_4 (Panreac, 96% wt.), $NaHCO_3$ (Merck), Na_2CO_3 (Panreac) and H_3PO_4 (Sigma-Aldrich, 85% wt.) were used for analysis purposes as well. All reagents were of analytical grade and used without further purification. Aqueous solutions were prepared using ultrapure water. Colorimetric indicator stripes were employed for tracing pH along reactions.

Reactors

MW-CWPO runs were performed in high pressure PTFE reaction vessels located in a microwave furnace (flexiWAVE, Milestone) equipped with optic fiber pyrometer, MW power (0-1.8 kW) and temperature controllers. The experiments were conducted in batch using 100 mL stoppered PTFE reactors which were initially loaded with aqueous pollutant solution (100 $mg \cdot L^{-1}$ phenol) and H_2O_2 (theoretical stoichiometric dose, that is 500 $mg \cdot L^{-1}$). Graphite was loaded initially at 500 $mg \cdot L^{-1}$. Heating rate was set at 80 $^oC \cdot min^{-1}$ to reach the reaction temperature 120 ºC, which was maintained for 60 minutes. During reaction, pressure rose up to 2.4 bar.

Non-MW CWPO runs were carried out in a pressured, jacketed glass tank reactor with a 500 mL volume that works up to 6 bar and 180 ºC. Reactor was initially loaded with water and 500 $mg \cdot L^{-1}$ graphite. Phenol and H_2O_2 were added right after reaching the operating temperature in order to avoid phenol decomposition over graphite in the heating step.

Analytical methods

Samples were periodically withdrawn from the reactors, placed in an ice bath to quench the reaction and immediately analyzed, after filtration through fiber glass filters (Albet FV-C), for tracing the reaction progress. For each sample aromatics, short-chain acids, TOC and H_2O_2 concentrations were measured.

Phenol, as well as aromatic and chloroaromatic intermediates were identified and quantified by means of a High Performance Liquid Chromatography (HPLC) (Pro Star 240, Varian) with a Diode Array detector. A C18 column (ZORBAX Eclipse Plus C18, 100 mm, 1.8 µm) was used as stationary phase and a 4 mM H_2SO_4 aqueous solution at 1 $mL \cdot min^{-1}$ as mobile phase. UV detector at 210 nm wavelength was used for phenol, resorcinol, catechol and hydroquinone and at 246 nm for p-benzoquinone. Chloroaromatics were analyzed using a C18 column (ZORBAX Eclipse Plus C18, 100 mm, 1.8 µm) as stationary phase and an acetonitrile/acetic acid (75mM, 50/50) solution at 0.8 $mL \cdot min^{-1}$ as mobile phase. UV detector was set at 270 nm.

Quantification of chloride, as well as short-chain organic acids were analyzed by an ion chromatograph with chemical suppression (Metrohm 790 IC) using a conductivity detector. A Metrosep A supp 5–250 column (25 cm length, 4 mm internal diameter) was used as stationary phase and 0.7 $mL \cdot min^{-1}$ of a 3.2 mM/1 mM aqueous solution of Na_2CO_3 and $NaHCO_3$, respectively, as mobile phase. Total Organic Carbon was measured using a TOC analyzer (Shimadzu TOC-VSCH). Finally, residual H_2O_2 in liquid phase was determined by colorimetric titration with a Cary 60 UV-Vis Agilent spectrophotometer using the $TiOSO_4$ method (Eisenberg 1943).

Results

The results of this research may be divided into three stages: screening to find optimal operation conditions, influence of salinity and kinetic calculations.

MW-CWPO optimization

Previous research of the group, in which several carbonaceous materials were tested, proved that 100 mg·L^{-1} phenol can be completely depleted in MW-CWPO using 500 mg·L^{-1} Sigma-Aldrich graphite as catalyst at stoichiometric dosage of H_2O_2 (500 mg·L^{-1}), 120 ºC and pH_0 value of 3. In order to perform an optimization of the operating conditions of the process, these parameters are varied according to the plan that shows Table 1. In bold is remarked the variable that changes for each specific run.

Table 1. Main variables and its values for the different runs.

Run	[H_2O_2] (mg·L^{-1})	[Graphite] (mg·L^{-1})	T (ºC)	pH_0
1	500	500	120	3
2	**250**	500	120	3
3	500	**1000**	120	3
4	500	500	**100**	3
5	500	500	120	**6**

The plan consists in varying just one parameter at a time in order to observe the effect of the changed variable on the process. Total Organic Carbon and H_2O_2 concentrations are traced for 60 minutes in order to study the effect of these variables on the reaction. Results are shown in Figure 2.

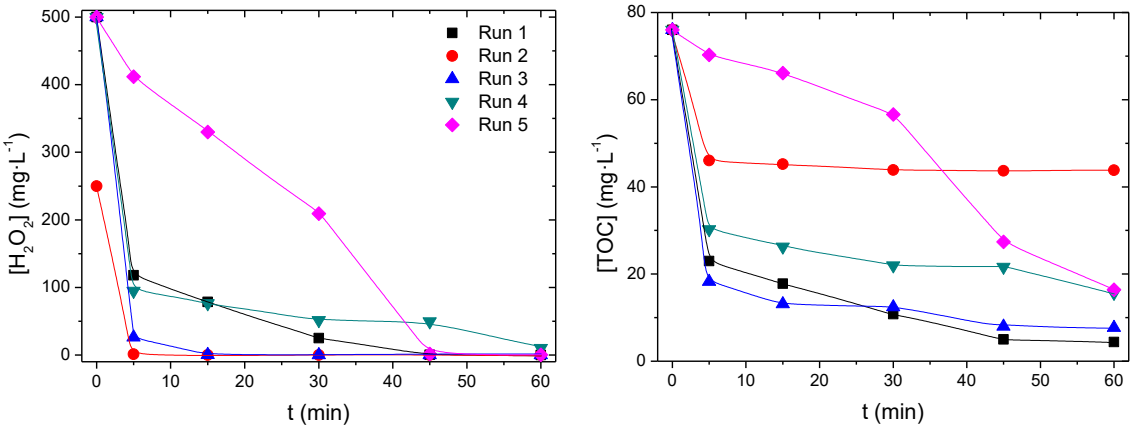

Figure 2. H_2O_2 and TOC evolution during reaction.

As Figure 2 depicts, the variation of reaction parameters in respect to Run 1 in general does not come up as an advantageous alternative. Fastest runs correspond to high catalyst and low H_2O_2 concentrations (Runs 2 and 3). These occur nearly at same rate, since catalyst to oxidant ratio is the same for both, although the reduction of 50% the stoichiometric H_2O_2 dosage in Run 2 renders a TOC oxidation limited to 40%. The slowest run is the one at pH_0 close to neutral (Run 5), but as reaction proceeds, short chain acids are generated, lowering the pH in the reaction media and enhancing both H_2O_2 consumption and TOC removal. The basification to pH 6 slows down the reaction, since neither H_2O_2 nor TOC decomposition are favored at such conditions and although H_2O_2 is finally fully converted, the final mineralization degree is lower due to hydroxyl and hydroperoxyl radical recombination at circumneutral pH yielding water and oxygen. Results are quantitatively alike to those of 100 ºC reaction (Run 4), but the latter occurs faster because the acidic medium favors hydroxyl radicals usage. All the three yield to lower mineralization than reactions at Runs 1 and 3, decomposing both nearly 90% TOC with a 100% H_2O_2 conversion.

One of the key parameters in CWPO is H_2O_2 consumption, as it the represents the highest operating cost. In order to verify this parameter, Figure 3 shows TOC conversion versus H_2O_2 conversion in relation to the stoichiometric amount. In these conditions, the diagonal represents the ideal behavior of the system. Points above the diagonal correspond to pollutant or intermediates adsorption, with a higher TOC removal than that theoretical according to the stoichiometry of the reaction. On the other hand, points below the diagonal are related to a non-efficient oxidation, with less mineralization than expected. Thus, the data closest to the diagonal represents the most efficient process.

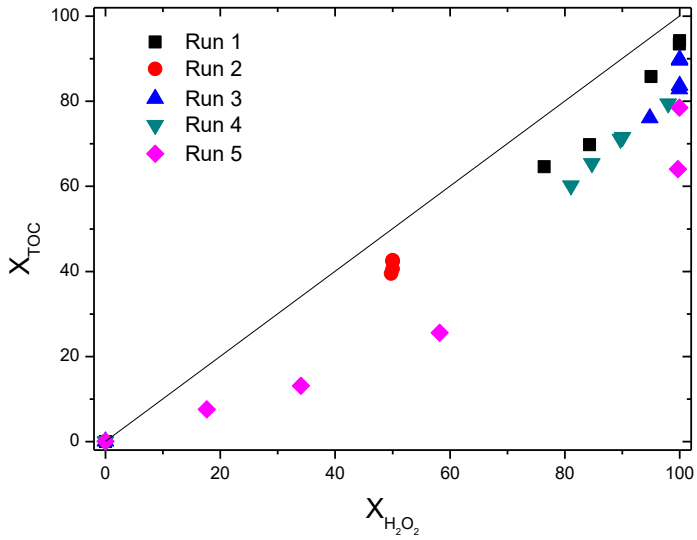

Figure 3. H_2O_2 consumption efficiency related to TOC conversion for all runs depicted in Table 1.

Figure 3 shows that the most efficient alternative in terms of H_2O_2 exploitation is the one happening at Run 1, although similar result is achieved at 1000 $mg \cdot L^{-1}$ catalyst. In addition, the consequence of halving stoichiometric H_2O_2 dosage is similar to lowering reaction temperature to 100ºC. Finally, the least efficient alternative is the one that runs at pH 6, (Run 5), results that concur with those extracted from Figure 2.

It is widely known that phenol oxidation pathway entails formation of aromatic diol isomers hydroquinone, resorcinol and catechol, followed by the most oxidized form of ring, *p*-benzoquinone. Further oxidation yields the ring opening and formation of short chain acids: acetic, formic, malonic, maleic, fumaric and oxalic acids (J.A. Zazo 2005). The importance of tracing these compounds resides in their toxicity, especially of *p*-benzoquinone (J. A. Zazo 2006). Hence, these intermediates were followed during reaction and their concentrations are depicted within Figure 4-Figure 8.

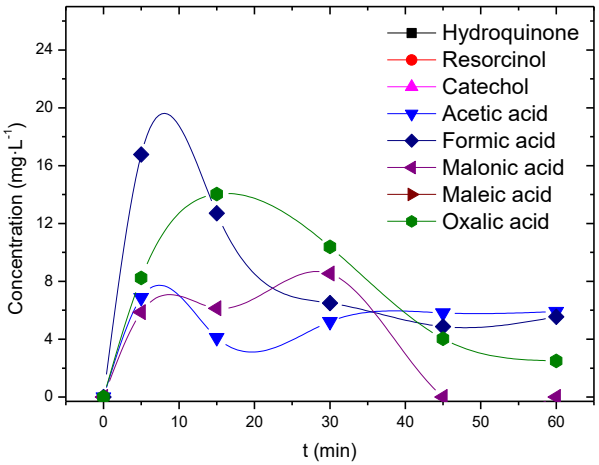

Figure 4. Identified intermediates evolution working at 500 mg·L^{-1} H_2O_2, 500 graphite, 120 ºC and pH_0 3 (Run 1).

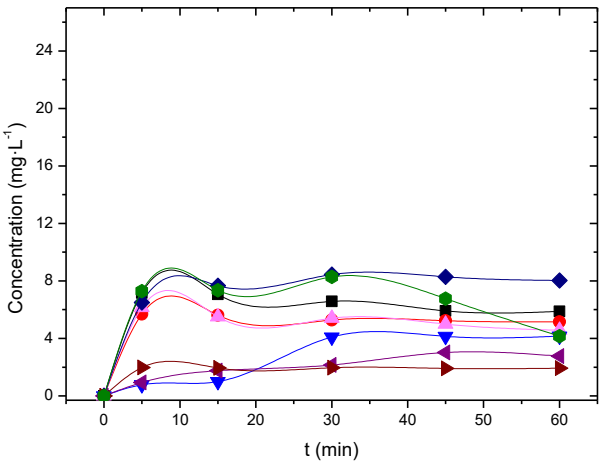

Figure 5. Identified intermediates evolution working at 250 mg·L^{-1} H_2O_2, 500 graphite, 120 ºC and pH_0 3 (Run 2).

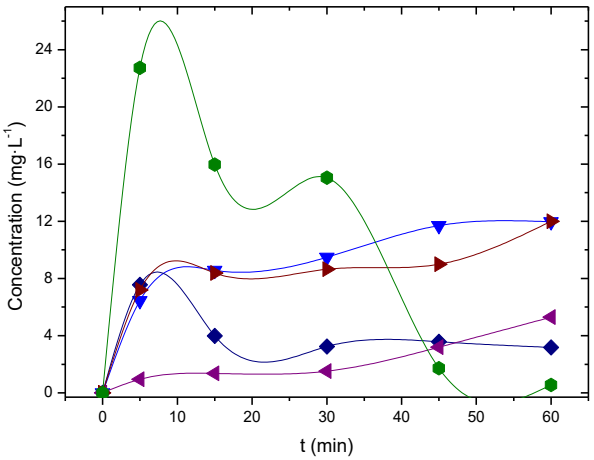

Figure 6. Identified intermediates evolution working at 500 mg·L^{-1} H_2O_2, 1000 graphite, 120 ºC and pH_0 3 (Run 3).

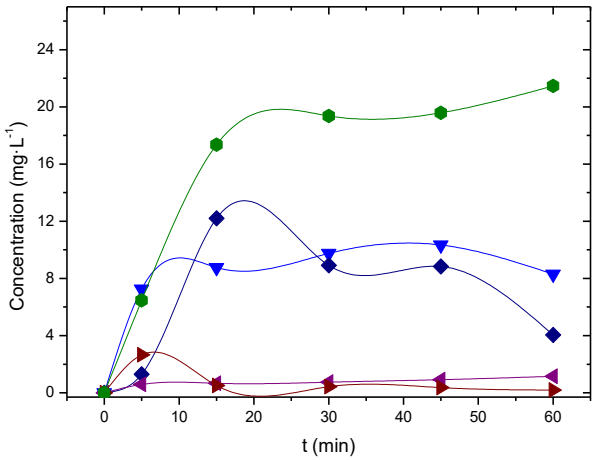

Figure 7. Identified intermediates evolution working at 500 mg·L^{-1} H_2O_2, 500 graphite, 100 ºC and pH_0 3(Run 4).

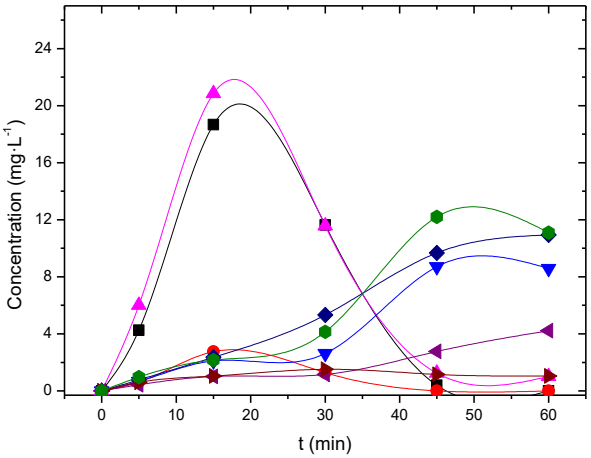

Figure 8. Identified intermediates evolution working at 500 mg·L^{-1} H_2O_2, 500 graphite, 120 ºC and pH_0 6 (Run 5).

Initial phenol hydroxylation takes place predominantly in *para* and *ortho* position, since hydroquinone and catechol are the most abundant aromatics. Nonetheless, these aromatic intermediates were only detected when working at under-stoichiometric H_2O_2 and at circumneutral starting pH. Short chain carboxylic acids as acetic, formic and oxalic appear at higher concentrations, proving to be more resistant to mineralization. There is a remarkably high oxalic acid concentration at the end of the fourth run. It turns out that oxalic is a recalcitrant acid that decomposes at high temperature and, according to Figure 7, 100ºC are not enough to achieve its complete removal.

Thus, the rest of the scenarios correspond to a quick ring opening yielding carboxylic acids or condensation byproducts. Several authors (J.A. Zazo 2005), (C. M. Dominguez 2014), (Díaz de Tuesta 2016) described the condensation of byproducts, which cannot be directly measured since they are normally adsorbed on the catalyst's surface, but can be quantified by a carbon balance. Said balance may be calculated once the foreseeable reaction intermediates are identified, determining the concentration of all species and comparing theoretical and measured TOC concentrations. The carbon balance evolution over reaction time for all the runs is shown within Figure 9-Figure 13 in the next page.

Condensation byproducts are formed in the early stages of reaction and can be completely oxidized when working at pH_0 3, 120ºC using the stoichiometric dose of H_2O_2, as can be seen in Runs 1 and 3 (Figure 9 and Figure 11). When working at sub-stoichiometric H_2O_2, a high amount of undesired condensation byproducts is generated, which are fairly stable, as they are not later eliminated by high temperature or hot spot formation on the surface of the catalyst, and remain in the medium, rising residual TOC concentration. Nonetheless, in presence of H_2O_2, condensation byproduct breakdown is strongly affected by temperature, as observed in Figure 12.

To sum up the results obtained so far, proposed treatment has proved to work for 100 $mg \cdot L^{-1}$ phenol aqueous effluent mineralization at 500 $mg \cdot L^{-1}$ graphite, stoichiometric H_2O_2 dosage, 120 °C and pH_0 3, without generating more toxic intermediates.

Yet the need of addressing seawater pollutants evidences the importance of effluents' salinity, which should not compromise the efficiency of this alternative.

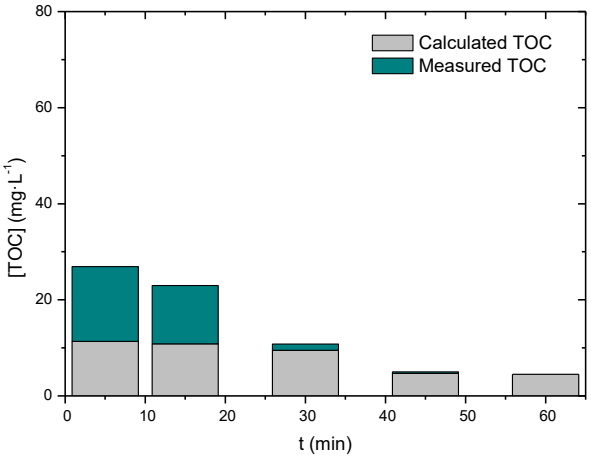

Figure 9. Calculated and measured TOC working at 500 mg·L^{-1} H_2O_2, 500 mg·L^{-1} graphite, 120 ºC and pH_0 3 (Run 1).

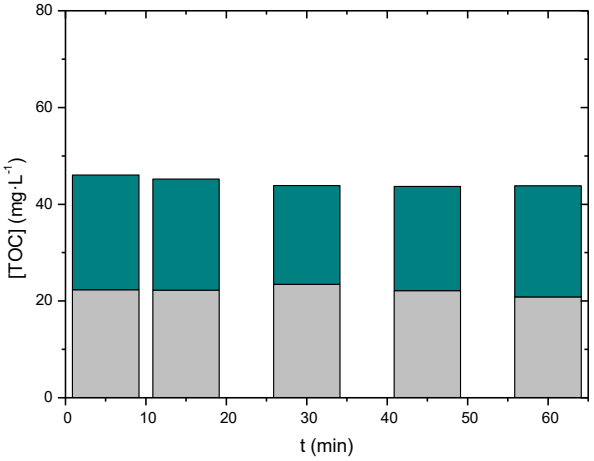

Figure 10. Calculated and measured TOC working at 250 mg·L^{-1} H_2O_2, 500 mg·L^{-1} graphite, 120 ºC and pH_0 3 (Run 2).

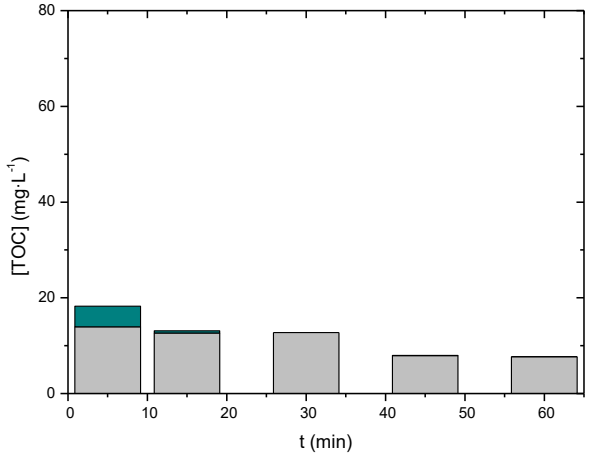

Figure 11. Calculated and measured TOC working at 500 mg·L^{-1} H_2O_2, 1000 mg·L^{-1} graphite, 120 ºC and pH_0 3 (Run 3).

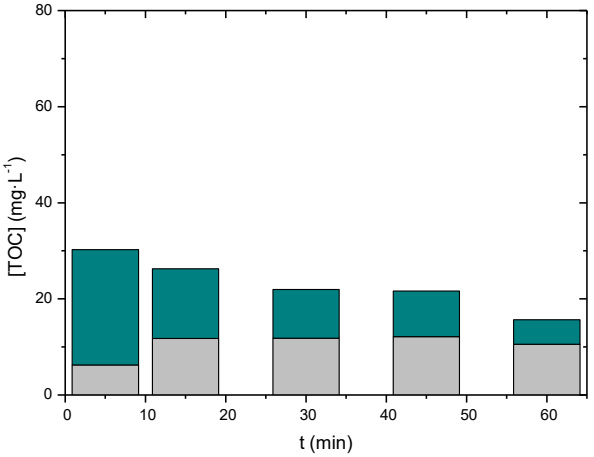

Figure 12. Calculated and measured TOC working at 500 mg·L^{-1} H_2O_2, 500 mg·L^{-1} graphite, 100 ºC and pH_0 3 (Run 4).

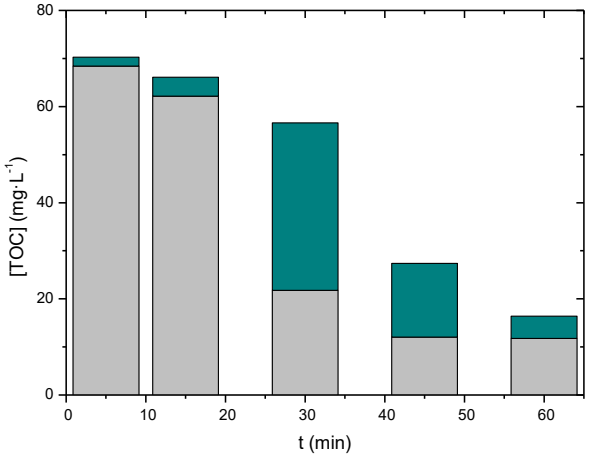

Figure 13. Calculated and measured TOC working at 500 mg·L^{-1} H_2O_2, 500 mg·L^{-1} graphite, 120 ºC and pH_0 6 (Run 5).

Influence of salinity in CWPO and MW-CWPO

As it has already been stated, operation variables, namely the concentration of phenol, addition of MW to CWPO treatment and concentration of chloride will be studied and developed within the following lines. Table 2 contains the characteristics of the reactions that will be executed to comprehend the influence of aforementioned variables. For each one of the four combinations, chloride anion is added as NaCl at [Cl^-] 1, 10, 25 and 40 $g \cdot L^{-1}$, in order to observe its impact and compare the results of corresponding runs with the blank, in which no chloride is added. Both [TOC] and [H_2O_2] are traced for comparison purposes.

Table 2. Experimental procedure for multivariable study.

Series	Pollutant	Technology	Chloride anion concentration
1	No phenol	CWPO	0, 1, 10, 25, 40 $g \cdot L^{-1}$
2		MW-CWPO	
3	100 $mg \cdot L^{-1}$ phenol	CWPO	
4		MW-CWPO	

According to Table 2, runs without phenol are carried out in order to study the influence of chloride in H_2O_2 decomposition. Afterwards, these will be compared to the results obtained in the presence of phenol.

For the first and second runs, both blanks, H_2O_2 concentration evolves as depicted in Figure 14 in a CWPO system and per Figure 15 in MW-CWPO.

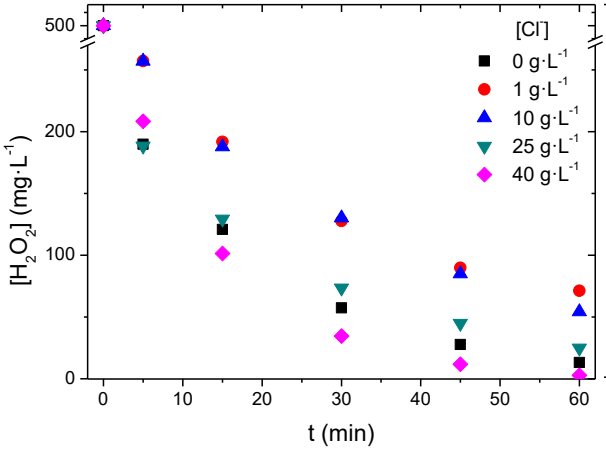

Figure 14. H_2O_2 evolution in CWPO without phenol.

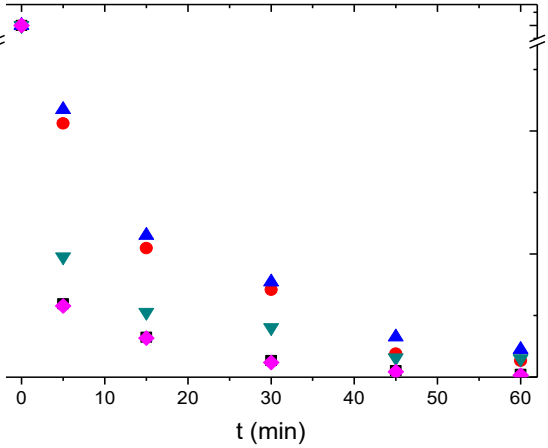

Figure 15. H_2O_2 evolution in MW-CWPO without phenol.

In absence of phenol, for both CWPO and MW-CWPO, there is not a clear tendency related to the addition of chloride. Nonetheless, it should be noted that Cl^- concentrations up to 10 $g \cdot L^{-1}$ have a negative effect over the reaction, since they slow down H_2O_2

decomposition, whereas higher concentrations result in a similar trend to the one observed in absence of chloride. In fact, in MW-CWPO H_2O_2 decomposition rate is alike at extreme Cl^- concentrations (0, 40 $g \cdot L^{-1}$). The cause of this phenomenon is that, at low concentrations, chloride anions compete with H_2O_2 in the catalyst redox cycle. Thus, instead of decomposing H_2O_2, Cl yields $Cl^{\bullet}$, slowing H_2O_2 depletion. However, at higher concentrations (25-40 $g \cdot L^{-1}$) chloride ions are more likely to react with H_2O_2, yielding HClO, which empowers H_2O_2 decomposition rate.

Comparing both systems, H_2O_2 decomposition occurs at higher rate in the MW-assisted process. This can be attributed to hot spots formation, as mentioned in the introductory chapter. Thus, the additional heat favors the impetuous and rapid molecular motion (N. Remya 2011).

According to the *Experimental procedure* shown in Table 2, once the first and second runs have been carried out, phenol is added at 100 $mg \cdot L^{-1}$. In this case, H_2O_2 decomposes as depicted in Figure 16 for CWPO and as per Figure 17 for MW-CWPO.

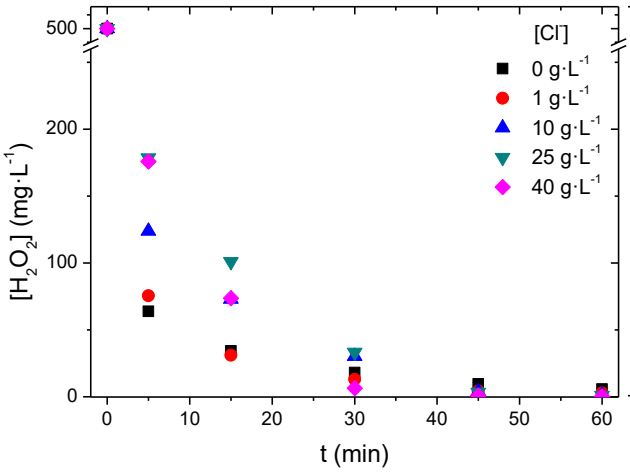

Figure 16. H_2O_2 evolution at CWPO, phenol system.

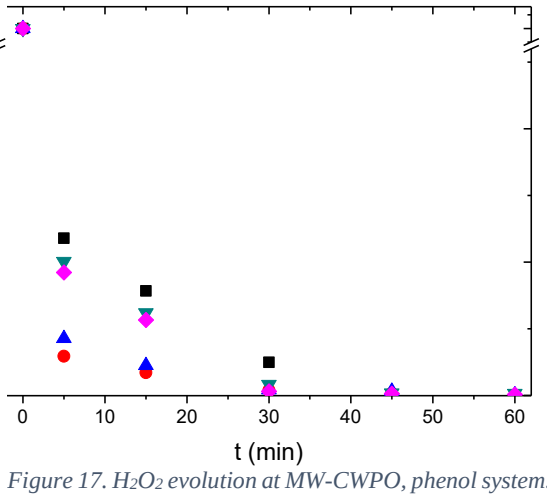

Figure 17. H_2O_2 evolution at MW-CWPO, phenol system.

For the CWPO treatment in presence of phenol, H_2O_2 decomposition rate does follow a tendency: the higher [Cl^-], the slower the initial reaction rate, due to the effect explained for absence of phenol. On the contrary, for the MW-CWPO system with phenol, there is not a clear tendency. Again, extreme [Cl^-] present similar decomposition rates, although contrarily to Figure 15, low Cl^- concentrations, (up to 10 $g \cdot L^{-1}$) seem to enhance H_2O_2 decomposition. Thus, in that range there is a synergic effect between chloride and organic matter, achieving a faster H_2O_2 conversion. When phenol is present, except for 40 $g \cdot L^{-1}$ Cl^-, the interaction between chloride and catalyst' surface accelerates the redox cycle. The reason for the empowerment of this effect could be a phenol-adsorption in graphite's

surface, which becomes altered by the action of chloride. Hence, adsorbed phenol remains closer to the catalyst, accelerating the oxidation reaction, phenomenon that has already been observed for other processes, as mentioned in the introductory chapter (R. Yuan 2012). For high chloride concentrations, it evolves slower than in homologous non-phenol case since relative amounts of H_2O_2 and Cl^- in the media is lower.

In order to verify the previous hypothesis, organic matter decomposition must be studied. In addition, it is a key parameter for evaluating wastewater treatments, as long as initial pollutant may be oxidized, but to other more toxic compounds, which would have an impact on TOC measure. Hence, Figure 18 shows TOC evolution in CWPO, whereas Figure 19 corresponds to MW-CWPO system.

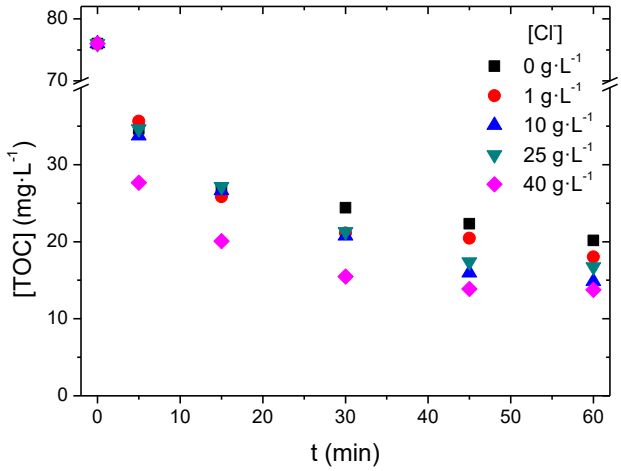

Figure 18. TOC evolution at CWPO, phenol system.

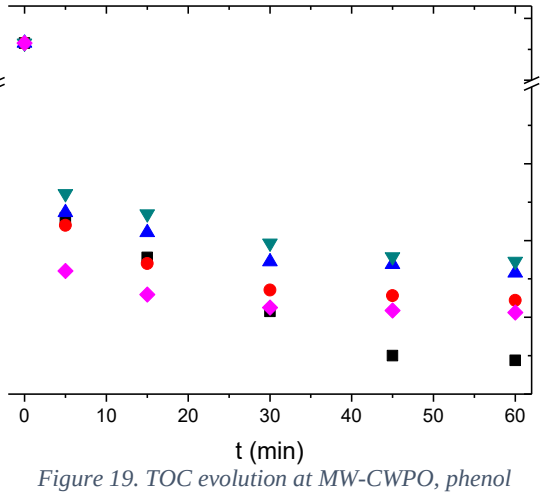

Figure 19. TOC evolution at MW-CWPO, phenol system.

In CWPO, TOC degradation is enhanced at high [Cl^-], contrary to H_2O_2 decomposition, that slowed down as [Cl^-] grew. At low chloride concentrations (0-25 $g \cdot L^{-1}$), TOC evolution results vary slightly. Opposed to CWPO, for most of the cases in the MW-CWPO system –except for 40 $g \cdot L^{-1}$– an augmentation of [Cl^-] lowers TOC decomposition efficiency. In fact, the run with no salt in the reaction matrix, despite presenting a lower initial rate, yields the maximum mineralization degree. This trend has no correspondence with H_2O_2 decomposition observed in Figure 17. As it can be noticed, the already mentioned strengthen effect of phenol adsorption at high Cl^- concentrations could be confirmed by these runs, with phenol removal being enhanced in CWPO but not in MW-CWPO. This crossed effect could be due to the fact that MW-CWPO already worked efficiently before addition of chloride. Finally, in MW-CWPO phenol removal is faster than CWPO, which demonstrates the advantageous effect of hot spots.

With the aim of determining the breakthrough that the process experiences with MW, efficiencies in CWPO and MW-CWPO are compared. Figure 20 and Figure 21 depict H_2O_2 versus TOC depletion for both processes.

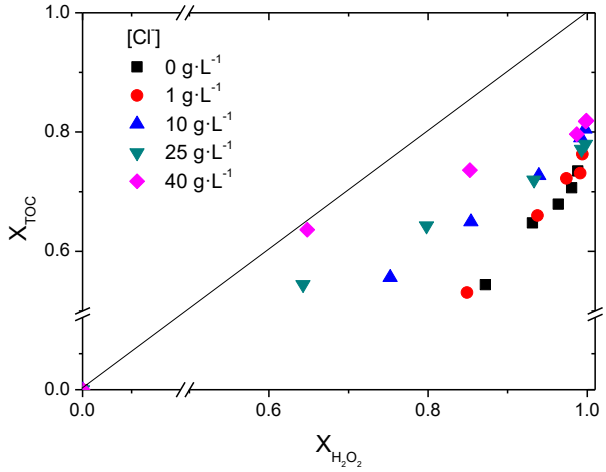

Figure 20. TOC versus H_2O_2 conversion for CWPO, phenol system.

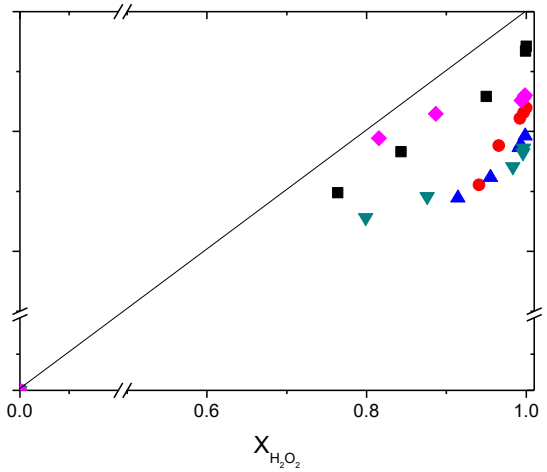

Figure 21. TOC versus H_2O_2 conversion for MW-CWPO, phenol system.

The acceleration of TOC depletion that has already been observed in a CWPO system with the addition of Cl^- turns effectively into an enhancement of the reaction efficiency for lower H_2O_2 conversions, as shown in Figure 20. Nevertheless, as long as reaction progresses, differences tend to diminish.

When MW are introduced in the process, efficiency is enhanced, especially at low Cl^- concentrations (0 and 10 $g \cdot L^{-1}$), which turned out to be the slowest in CWPO system. Anyhow, yet the lowest mineralization for MW-CWPO, which corresponds to 25 $g \cdot L^{-1}$ Cl^- run, comes to 77% TOC removal, being the most unfavorable case. This outstanding result means that this process represents a feasible alternative to remove pollutants in aqueous phase in spite of the presence of salts in the matrix. Likewise, literature already announced that combined method of MW/catalyst/H_2O_2 is much more effective toward phenol degradation than using MW alone, catalyst alone, MW/catalyst, MW/H_2O_2, and catalyst/H_2O_2 methods combinations (Z. Liua 2018).

Gathering all the results related to the presence of chloride, chloride anion at low concentrations might act as hydroxyl radicals scavenger. They react with all kind of generated radicals, including $HO^{\bullet}$ (Eq. 7), preventing it from oxidizing organic matter. Actually, chloride anions can oxidize organic matter as well, but less efficiently, as depicted in Figure 18 and Figure 19. However, at a sufficiently high concentration, they might contribute to pollutant oxidation. As per Figure 17, the reaction that decomposes

H_2O_2 more slowly turns out to be mineralizing more TOC. Gathering results from Figure 20 and Figure 21, H_2O_2 is highly efficient when chloride anion concentration is elevated. The reason is that when [Cl^-] is 40 $g \cdot L^{-1}$, graphite's surface is altered, provoking that phenol is adsorbed, close to catalyst, favoring the oxidation reaction and H_2O_2 redox cycle rather than the Cl^- radical scavenging reaction. Actually, albeit having nonpolar sp^2 carbon structure, graphite is mildly hydrophilic, but principally hydrophobic (A. Kozbial 2016). Therefore, this change of the chemical potential is a boost for reaction. At the same time, regarding TOC decomposition, chloride anion may act as a $HO^{\bullet}$ scavenger at low concentrations, since the effect of catalyst's surface change, especially in no-phenol cases is not enough to overcome the detrimental effect of scavenging. This phenomenon can also be explained in terms of reaction mechanisms.

Graphite is capable of accepting and donating electrons. This amphoteric character, equally attributable to H_2O_2, enables the system to work cyclically (Figure 22). Mineralization is possible because of the radical attack that suffers organic matter. Radicals are generated when H_2O_2 is reduced by taking an electron from the graphite surface, yielding $HO^{\bullet}$. The cycle can be closed via H_2O_2 oxidation, transferring an electron to the graphite surface, generating $HOO^{\bullet}$.

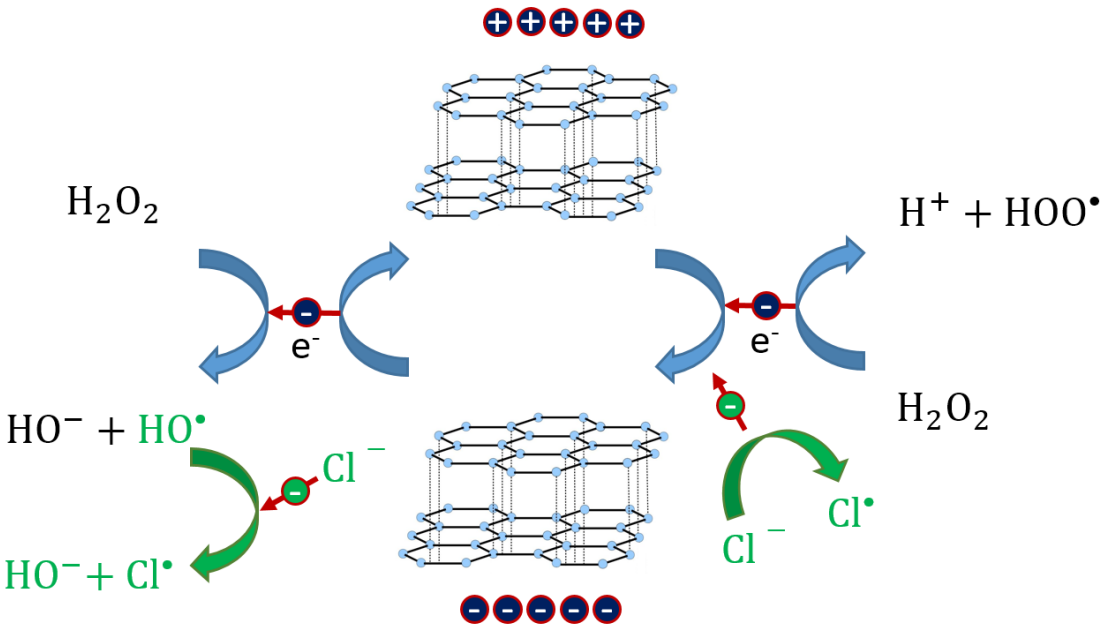

Figure 22. Schematics for redox cycle between graphite and H_2O_2 (Own elaboration).

When chloride anions take part in the reaction, an electron is released (Eq. 12). This leaves the electron balance altered, causing the cycle between H_2O_2 and $HOO^{\bullet}$ not to

close, since catalyst is positively charged and cannot donate the electron to H_2O_2 molecule. Reactions of chloride anions and chlorine-water combination occur as well (Eq. 11 and Eq. 13, respectively). Reactions occurring in presence of chloride are marked in green in Figure 22.

$$HO^{\bullet} + Cl^{-} \rightarrow Cl^{\bullet} + HO^{-} \qquad \textit{Eq. 12}$$

$$Cl_2 + H_2O \rightarrow HClO + HCl \qquad \textit{Eq. 13}$$

In any case, it is important that the selected treatment does not cause toxic compounds; in this particular case, chlorinated organic molecules are potentially dangerous.

For all the previous reactions, pH was constant around initial value of 3, meaning that the system was run under control and operating at its optimum. The fact that pH does not increase is a sign that no chlorinated compounds are being formed. Moreover, it has been observed for all the reactions that phenol was completely depleted after 5 minutes. This quick oxidation of phenol and aromatic byproducts would prevent any chance of chloroaromatics formation. Furthermore, HPLC analysis revealed that no chlorine-containing organic compounds were present in the effluents. Consequently, chloride in the aqueous matrix does not enter the organic molecules. Thus, remaining TOC can be ascribed to non-chlorinated and, therefore, less toxic compounds.

Nevertheless, a balance of chloride is calculated to have an idea of the fate of chloride introduced in the system along the reaction. Following the same order as for other discussed variables, according to Table 2, evolution of chloride is initially evaluated for CWPO and MW-CWPO cases without phenol, and afterwards for same reaction schemes and phenol-containing reactions. Figure 23-Figure 26 show the evolution of chloride over the reaction time for diverse salt concentrations.

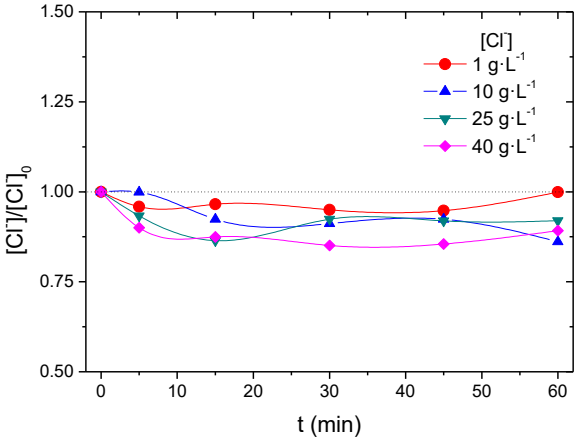

Figure 23. Chloride evolution along reaction in CWPO in absence of phenol.

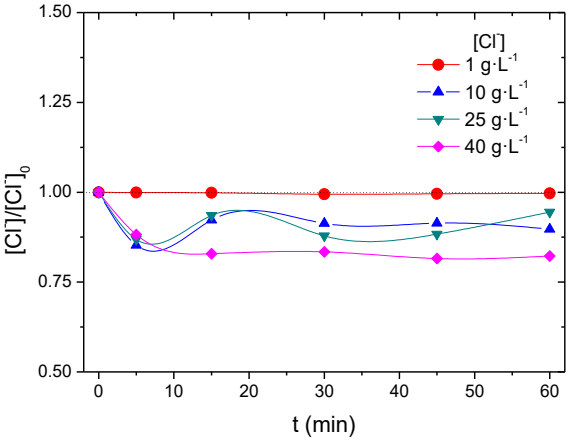

Figure 24. Chloride evolution along reaction in MW-CWPO in absence of phenol.

Figure 23 presents small deviations after reaction in respect to Cl^-/Cl^-_0 equal to one. The highest deviation is observed for 40 $g \cdot L^{-1}$ Cl^-, since in absence of organic matter, $HO^\bullet$ radicals attack chloride anions (Eq. 12), then chloride radicals are recombined (Eq. 11) and eventually cause reaction according Eq. 13 to occur, enhancing HClO formation.

Figure 24 shows how the relation Cl^-/Cl^-_0 increases when chloride anion concentration in the media is higher. This means that the highest HClO formation takes place at 40 $g \cdot L^{-1}$ Cl^- in MW-CWPO as well.

In short, chloride balance does not close in absence of phenol because part of chloride is in HClO form in both CWPO and MW-CWPO systems.

Lastly, once that the impact of chloride concentration has been studied for blank CWPO and MW-CWPO reactions, phenol is added to the system. Figure 25 and Figure 26 show chloride evolution for both systems.

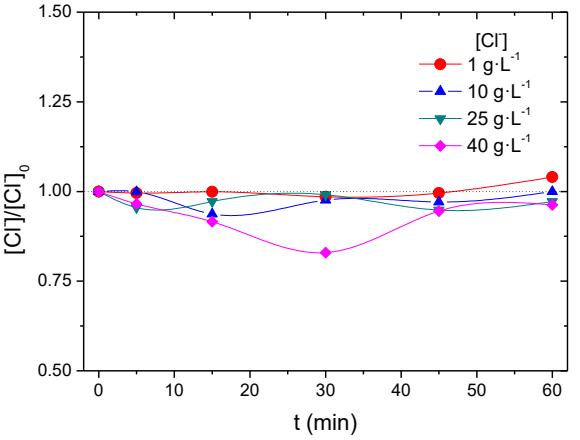

Figure 25. Chloride evolution along reaction in CWPO for phenol.

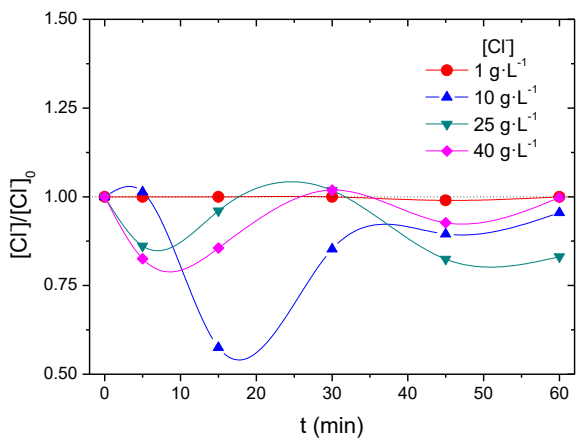

Figure 26. Chloride evolution along reaction in MW-CWPO for phenol.

As depicted in Figure 25, chloride anion ends at the same concentration and form as was added to the system for all chloride concentrations. That means that it neither does turn into HClO form, nor introduced into reaction byproducts. Instead, after Eq. 12, HO^- reacts with organic matter, impeding Eq. 13 to take place. The highest deviation is obtained for 40 $g \cdot L^{-1}$, that shows a peak at reaction halfway, however after reaction is not observed anymore.

According to Figure 26, there is a general divergence during the first half of the reaction, but it ceases after all reactions, meaning that chloride balances close at the end for all the reactions except for the 25 $g \cdot L^{-1}$ run, which is close (around Cl^-/Cl^-_0 equal to 0.85).

In conclusion, for all the reactions chloride anion concentration does not deviate significantly from initial. Especially in reactions occurring in absence of phenol, chloride balance deviation is higher because of HClO formation. Nevertheless, in presence of phenol, final form is Cl^-, so Cl- balance adds up at 60 min.

Kinetics

Reactions corresponding to the four series presented in Table 2 (0/100 $mg \cdot L^{-1}$ phenol, CWPO/CWPO-MW, 0-40 $g \cdot L^{-1}$ Cl^-) were studied in order to obtain their kinetic constants. Both H_2O_2 and TOC were fitted using an integral approach, proving to be properly modelled by an integer kinetic order.

Firstly, H_2O_2 decomposition can be described by a pseudo-first order kinetics as depicted in Eq. 14.

$$\left(-r_{H_2O_2}\right) = -\frac{dC_{H_2O_2}}{dt} = k \cdot C_{H_2O_2} \qquad \textit{Eq. 14}$$

Table 3 gathers kinetic constants and fitting parameters.

Table 3. Kinetic constants and regression coefficients for H_2O_2 decomposition at diverse conditions.

$[Cl^-]$ $(g \cdot L^{-1})$	no phenol				phenol			
	S1. CWPO		S2. MW-CWPO		S3. CWPO		S4. MW-CWPO	
	k (min^{-1})	r^2	k (min^{-1})	r^2	k (min^{-1})	r^2	k (min^{-1})	r^2
0	0.08	0.98	0.13	0.93	0.13	0.90	0.16	0.93
1	0.05	0.96	0.08	0.97	0.15	0.95	0.09	0.99
10	0.05	0.96	0.08	0.97	0.10	0.97	0.17	0.93
25	0.07	0.96	0.11	0.90	0.09	0.98	0.16	0.92
40	0.08	0.99	0.13	0.94	0.17	0.99	0.14	0.90

Comparing CWPO to MW-CWPO, for *Series 1* and *2*, which were carried out in absence of phenol, the latter run is faster due to MW hot spots formation. Consequently, apparent rate constants are on average a 57% higher for *Series 2*. Whereas for phenol-containing *Series 3* and *4*, they are also a 13% higher in the latter, meaning that MW hot spots are equally speeding the reaction in the presence of phenol.

Comparing phenol and no-phenol runs, relative to H_2O_2 decomposition apparent rate constant, it is in a range of 0.05-0.13 min^{-1} for *Series 1* and *2*, and slightly higher, 0.09-0.17 min^{-1}, for *Series 3* and *4*. Nevertheless, on average they have values alike (0.13 and 0.14 min^{-1}, respectively).

As it can be noticed, the apparent rate constant is sensitive to chloride concentration. The differences between constants corresponding to different $[Cl^-]$ is 40-50%, but impact of $[Cl^-]$ is not a direct relation, since it does not follow a strict tendency with the addition of chloride.

Secondly, TOC decomposition reaction was addressed for obtaining its kinetic parameters. As it was already mentioned, this is the parameter that determines the real efficiency of the treatment. TOC decomposition can be described by a pseudo-second order kinetics as depicted in Eq. 15.

$$(-r_{TOC}) = -\frac{dC_{TOC}}{dt} = k \cdot C_{TOC}{}^2 \qquad \textit{Eq. 15}$$

Table 4 shows kinetic constants and fitting parameters.

Table 4. Kinetic constants and regression coefficients for TOC mineralization at diverse conditions.

$[Cl^-]$ $(g \cdot L^{-1})$	S3. CWPO		S4. MW-CWPO	
	k $(L \cdot min \cdot mg^{-1}) \cdot 10^3$	r^2	k $(L \cdot min \cdot mg^{-1}) \cdot 10^3$	r^2
0	1.15	0.90	2.74	0.96
1	1.39	0.94	2.57	0.92
10	1.43	0.97	1.79	0.85
25	1.44	0.97	1.55	0.87
40	2.29	0.97	3.24	0.84

The range of apparent kinetic constants for TOC mineralization is significantly higher in all cases under MW-CWPO. Furthermore, the apparent rate constant when there is a MW supply is a 60% higher than the average for CWPO ($2.4 \cdot 10^{-3}$ versus $1.5 \cdot 10^{-3}$ $L \cdot min \cdot mg^{-1}$). The apparent rate constant for TOC removal is even more sensitive to chloride concentration, with a difference higher than 50% for different $[Cl^-]$, and again it does not follow a strict tendency with the addition of chloride.

Conclusions

- Proposed treatment has proved to work for 100 $mg \cdot L^{-1}$ phenol aqueous effluent mineralization at 500 $mg \cdot L^{-1}$ graphite, stoichiometric H_2O_2 dosage, 120 °C and pH_0 3, at different Cl^- concentrations (0-40 $g \cdot L^{-1}$) without chlorinated aromatic intermediates formation.
- It has been demonstrated that adding MW as energy source to a CWPO system represents a breakthrough regarding organic matter depletion efficiency in saline matrices.
- At low chloride concentrations, scavenging phenomena hinder the reaction, decreasing its efficiency.
- However, high chloride concentrations provoke a change in the surface of catalyst that approaches reactants to active centers, activating the reaction again.
- The presence of chloride anion does not cause chlorinated organic compounds neither in CWPO nor in MW-CWPO.
- Apparent rate constant for H_2O_2 decomposition is, on average, around 0.13 min^{-1} and $1.54 \cdot 10^{-3}$ $L \cdot min \cdot mg^{-1}$ for TOC mineralization in CWPO whereas for MW-CWPO 0.14 min^{-1} and $2.38 \cdot 10^{-3}$ $L \cdot min \cdot mg^{-1}$, respectively.

References

A. Kozbial, F. Zhou, Z. Li, H. Liu, L. Li. "Are Graphitic Surfaces Hydrophobic?" *Accounts of Chemical Research, 49*, 2016: 2765-2773.

A. L. Garcia-Costa, J.A. Zazo, J.J. Rodriguez, J.A. Casas. "Microwave-assisted catalytic wet peroxide oxidation. Comparison of Fe catalysts supported on activated carbon and gamma-alumina." *Applied Catalysis B: Environmental, 218*, 2017: 637-642.

A.L. Garcia-Costa, J.A. Zazo, J.A. Casas, J.J. Rodriguez. *Microwave-assisted advanced oxidation of petrochemical wastewater.* Abstract, San Francisco: Environmental Division 2016 - Core Programming Area at the 2016 AIChe Annual Meeting, 2016.

C. M. Dominguez, P. Ocón, A. Quintanilla, J.A. Casas, J.J. Rodriguez. "Graphite and carbon black materials as catalysts for wet peroxide oxidation." *Applied Catalysis B: Environmental, 144*, 2014: 599-606.

C.B. Molina, J.A. Zazo, J.A. Casas, J.J. Rodriguez. "CWPO of 4-CP and industrial wastewater with Al–Fe pillared clays." *Water Science and Technology, 61*, 2010: 2161-2168.

C.E. George, G.V.N. Rao, V. Thalakola. "Thermal desorption of contaminants using microwave heated rotary mixture." *Proceedings of the 29th Microwave Power Symposium.* Chicago, IL, 1994.

C.M. Dominguez, P. Ocon, A. Quintanilla, J.A. Casas, J.J, Rodriguez. "Highly efficient application of activated carbon as catalyst for wet peroxide oxidation." *Applied Catalysis B: Environmental*, 2013: 663-670.

D.A. Jones, T.P. Lelyveld, S.D. Mavrofidis, S.W. Kingman, N.J. Miles. "Microwave heating applications in environmental engineering - A review." *Resources, Conservation and Recycling, 34*, 2002: 75-90.

D.M. Gu, Y.Y. Chu, Z.B. Wang, Z.Z. Jiang, G.P. Yin, Y. Liu. "Methanol oxidation on Pt/CeO2-C electrocatalyst prepared by microwave-assisted ethylene glycol process." *Applied Catalysis B, 102*, 2011: 9-18.

Díaz de Tuesta, JL. *Modelización cinética y simulación de procesos de oxidación húmeda con peróxido de hidrógeno catalizada por negros de humo dopados.* Madrid: Universidad Autónoma de Madrid, 2016.

E. Cigdem, P. Audrey, M. Juan. "Synergetic pretreatment of sewage sludge by microwave irradiation in presence of H2O2 for enhanced anaerobic digestion." *Water Resources, 42*, 2008: 4674–4682.

E. Guélou, J. Barrault, J. Fournier, J.M. Tatibouët. "Active iron species in the catalytic wet peroxide oxidation of phenol over pillared clays containing iron." *Applied Catalysis B: Environmental, 44*, 2003: 1-8.

Eisenberg, G.M. "Colorimetric determination of hydrogen peroxide." *Industrial & Engineering Chemistry Analytical, 15*, 1943: 327-328.

F. Béguin, E. Frackowiak. *Carbons for Electrochemical Energy Storage and Conversion Systems.* Boca Raton, FL: CRC Press, 2009.

Fenton, H.J.H. "Oxidation of tartaric acid in presence of iron." *Journal of the Chemical Society, 65*, 1894: 899-910.

G. Pliego, J.A. Zazo, P. Garcia-Munoz, M. Munoz, J.A. Casas, J.J. Rodriguez. "Trends in the Intensification of the Fenton Process for Wastewater Treatment: An Overview." *Critical Reviews in Environmental Science and Technology, 45*, 2015: 2611-2692.

H. Hidaka, A. Saitou, H. Honjou, K. Hosoda, M. Moriya, N. Serpone. "Microwave-assisted dechlorination of polychlorobenzenes by hypophosphite anions in aqueous alkaline media in the presence of Pd-loaded active carbon." *Journal of Hazardous Materials, 148*, 2007: 22-28.

H. Le Chatelier, O. Boudouard. "Limits of Flammability of Gaseous Mixtures." *Bulletin de la Société Chimique de France, 19*, 1898: 483-488.

Haque, K.E. "Microwave energy for mineral treatment processes - A brief review." *International Journal of Mineral Processing*, 1999: 1-24.

I. Milosevic, H. Jouni, C. David, F. Warmont, D. Bonnin, L. Motte. "Facile microwave process in water for the fabrication of magnetic nanorods." *Journal of Physical Chemistry C, 115*, 2011: 18999-19004.

J. A. Zazo, J.A. Casas, A.F. Mohedano, J.J. Rodriguez. "Catalytic wet peroxide oxidation of phenol with a Fe/active carbon catalyst." *Applied Catalysis B: Environmental, 65*, 2006: 261-268.

J. Hong, N.N. Yuan, Y.X. Wang, S.H. Qi. "Efficient degradation of Rhodamine B in MW-H2O2 system at alkaline pH." *Chemical Engineering Journal, 191*, 2012: 364-368.

J.A. Menéndez, A. Arenillas, B. Fidalgo, Y. Fernández, L. Zubizarreta, E.G. Calvo. "Review: microwave heating processes involving carbon materials." *Fuel Processing Technolgy, 91*, 2010: 1-8.

J.A. Zazo, J.A. Casas, A.F. Mohedano, M.A. Gilarranz, J.J. Rodriguez. "Chemical Pathway and Kinetics of Phenol Oxidation by Fenton's Reagent." *Environmental Science & Technology, 39*, 2005: 9295-9302.

L. Yang, Z.L. Chen, J.F. Yang, Y. Liu, J. Wang, Y.J. Yu, X.M. Gao. "Removal of volatile fatty acid in landfill leachate by the microwave-hydrothermal method." *Desalination and Water Treatment, 52*, 2014: 4423-4429.

L. Zhang, X. Guo, F. Yan, M. Su, Y. Li. "Study of the degradation behavior of dimethoate under microwave irradiation." *Journal of Hazardous Materials, 149*, 2007: 675-679.

M. Munoz, Z.M. de Pedro, J.A. Casas, J.J. Rodriguez. "Improved wet peroxide oxidation strategies for the treatment of chlorophenols." *Chemical Engineering Journal, 228*, 2013: 646-654.

M. Ravera, A. Buico, F. Gosetti, C. Cassino, D. Musso, D. Osella. "Oxidative degradation of 1,5-naphthalenedisulfonic acid in aqueous solutions by microwave irradiation in the presence of H2O2." *Chemosphere 74*, 2009: 1309–1314.

M.C. Lu, J.N. Chen, C.P. Chang. "Effect of inorganic ions on the oxidation of dichlorvos insecticide with Fenton's reagent." *Chemosphere, 35 (10)*, 1997: 2285-2293.

N. Li, P. Wang, C. Zuo, H.L. Cao, Q.S. Liu. "Microwave-enhanced Fenton process for DMSO-containing wastewater." *Environmental Engineering Science, 27*, 2010: 271-280.

N. Remya, J-G. Lin. "Current status of microwave application in wastewater treatment—A review." *Chemical Engineering Journal, 166*, 2011: 797-813.

N. Wang, P. Wang. "Study and application status of microwave in organic wastewater treatment - A review." *Chemical Engineering Journal 283*, 2016: 193-214.

P. Müler, P. Klán, V. Církva. "The electrodeless discharge lamp: a prospective tool for photochemistry. Part 4: Temperature- and envelope material dependent emission characteristics." *Journal of Photochemistry and Photobiology A, 158*, 2003: 1-5.

Pignatello, J.J. "Dark and photoassisted Fe3+-catalyzed degradation of chlorophenoxy herbicides by hydrogen peroxide." *Environmental Science Technology, 26*, 1992: 944-951.

Pintar, A. "Catalytic processes for the purification of drinking water and industrial effluents." *Catalysis Today, 77*, 2003: 451-465.

R. Maciel, G.L. Sant'Anna Jr., M. Dezotti. "Phenol removal from high salinity effluents using Fenton's reagent and photo-Fenton reactions." *Chemosphere, 57*, 2004: 711-719.

R. Yuan, S. N. Ramjaun, Z. Wang, Jianshe Liu. "Photocatalytic degradation and chlorination of azo dye in saline wastewater: Kinetics and AOX formation." *Chemical Engineering Journal, 192*, 2012: 171-178.

S. Cataldo, A. Iannì, V. Loddo, E. Mirenda, L. Palmisano, F. Parrino, D. Piazzese. "Combination of advanced oxidation processes and active carbons adsorption for the treatment of simulated saline wastewater." *Separation and Purification Technology*, 2016: 101-111.

S. Lv, X. Chen, Y. Ye, S. Yin, J. Cheng, M. Xia. "Rice hull/MnFe2O4 composite: preparation, characterization and its rapid microwave-assisted COD removal." *Journal of Hazardous Materials, 171*, 2009: 634-639.

Sutton, W.H. "Microwave Processing of Ceramic Materials." *American Ceramic Society Bulletin, 68*, 1989: 376-386.

T.V.C.T. Chan, H.C. Reader. *Understanding Microwave Heating Cavities.* London: Artech House, 2000.

X.Y. Bi, H.Y. Yang, P.S. Sun. "Microwave-induced oxidation progress for treatment of imidacloprid pesticide wastewater." *Applied Mechanics and Materials, 229-231*, 2012: 2489-2492.

Z. Liua, H. Meng, H. Zhang, J. Cao, K. Zhou, J. Lian. "Highly efficient degradation of phenol wastewater by microwave induced H2O2-CuOx/GAC catalytic oxidation process." *Separation and Purification Technology*, 2018: 49-57.

Images:

http://www.electroboom.com/wp-content/uploads/2016/07/graphite-1024x1024.jpg

https://wiki.anton-paar.com/wp-content/uploads/05_microwave-heat-introduction.jpg